Proceeding of the 2004 American Control Conference
Boston, Massachusetts June 30 - July 2, 2004

Unicycles in Cyclic Pursuit

Joshua A. Marshall, Mireille E. Broucke, and Bruce A. Francis

Abstract— **In this paper, we study the geometric formations of multi-vehicle systems under a control law based on cyclic pursuit. The pursuit framework is particularly simple in that, for n ordered and identical wheeled vehicles, vehicle i simply pursues vehicle $i+1$ modulo n. We show that, for unicycles with constant speed, the multi-vehicle system's equilibrium formations are generalized regular polygons. We then study the local stability of these equilibrium polygons, revealing which formations are stable and which are not.**

I. INTRODUCTION

In this paper, we study a reconfiguration strategy for multi-vehicle systems based on the notion of *cyclic pursuit* from mathematics. From an engineering standpoint, the question of how to achieve desired *global* behaviours for multi-vehicle systems through the application of only simple and *local* interactions is of particular interest.

There has recently been great interest in this question. To name only a few results, Justh and Krishnaprasad [1] developed local steering laws for achieving both rectilinear and circular formations of planar multi-vehicle systems. Jadbabaie et al. [2] proved convergence results for a nearest-neighbour type problem, guaranteeing that all agents eventually move in an identical fashion, despite the distributed nature of their coordination law. Gazi and Passino [3] investigated aggregate behaviour in *swarms* of organisms, where operational models are analyzed for the purpose of potential engineering application. Sepulchre et al. [4] studied the connections between phase models of coupled oscillators and kinematic models of groups of agents.

Inspired by the so-called "bugs" problem from mathematics, we study the geometric formations of multi-vehicle systems under cyclic pursuit. The bugs problem refers to what is also known as the dogs, mice, ants, or beetles problem, and originally stems from the mathematics of *pursuit curves*, first studied by French scientist Pierre Bouguer (c. 1732). In 1877, Edouard Lucas asked, what trajectories would be generated if three dogs, initially placed at the vertices of an equilateral triangle, were to run one-after-the-other? Three years later, Henri Brocard replied with the answer that each dog's pursuit curve would be a logarithmic spiral and that the dogs would meet at a common point, known now as the *Brocard point* of a triangle. Consider n ordered bugs that start at the vertices of a regular n-polygon. If each bug pursues the next modulo n (i.e., *cyclic* pursuit) at constant speed, the bugs will trace out logarithmic spirals and eventually meet at the polygon's centre [5]. What happens if our n bugs do not start at the vertices of a regular n-polygon? This and other questions relating to the bugs problem have been asked and answered over time (e.g., [6], [7], [8]). Variations on the traditional problem have also been studied. For example, Bruckstein et al. [9] investigated both continuous and discrete pursuit, as well as both constant and varying speed scenarios.

Consider now a particular cyclic pursuit scheme where each "bug" is modelled as a kinematic unicycle. In this case, the unicycles will not generally be able to head towards their designated prey at each instant. What trajectories can be generated[1]? In this paper, we generalize the cyclic pursuit concept to nonholonomic vehicles and study its properties as a coordination algorithm for multi-vehicle systems. Thus, our primary motivation is to follow historical development and study the achievable formations for wheeled vehicles under cyclic pursuit. Alternatively, from a practical viewpoint, cyclic pursuit may be a feasible strategy for multi-vehicle systems since it is distributed (i.e., decentralized; no leader), scalable, and simple in that each agent is required to sense information from only one other agent. We study one particular control law that assumes each unicycle has the same constant forward speed, unlike in [10]. We show that the system's equilibrium formations are generalized regular polygons and we study their local stability.

II. UNICYCLE EQUATIONS OF PURSUIT

In this section, we briefly review some relevant results from [10]. Suppose there are n ordered vehicles, where each vehicle is a kinematic unicycle with nonlinear state model

$$\begin{bmatrix} \dot{x}_i \\ \dot{y}_i \\ \dot{\theta}_i \end{bmatrix} = \begin{bmatrix} \cos\theta_i & 0 \\ \sin\theta_i & 0 \\ 0 & 1 \end{bmatrix} \begin{bmatrix} v_i \\ \omega_i \end{bmatrix} = G(\theta_i)u_i, \qquad (1)$$

and where $[x_i, y_i]^\top \in \mathbb{R}^2$ denotes the i-th vehicle's position, $\theta_i \in \mathbb{R}$ is the vehicle's orientation, and $u_i = [v_i, \omega_i]^\top \in \mathbb{R}^2$ are control inputs. In this paper, we allow angles to take values in the set $\mathbb{R}$ to avoid a discontinuity in our feedback law, which depends on angles. Suppose vehicle i pursues the next, $i+1$, modulo[2] n.

Let r_i denote the distance between vehicle i and $i+1$, and let α_i be the difference between the i-th vehicle's heading and the heading that would take it directly towards its prey, $i+1$ (see Fig. 1). In the present paper, we fix each vehicle's forward speed and study the possible equilibrium formations when vehicle i's angular speed ω_i is assigned in direct proportion to the heading error α_i.

This research was funded in part by the Natural Sciences and Engineering Research Council of Canada (NSERC).

The authors are with the Department of Electrical and Computer Engineering, University of Toronto, 10 King's College Rd, Toronto, ON M5S 3G4, Canada (e-mail: {marshall,broucke,francis}@control.toronto.edu).

[1] We first asked this question in [10].

[2] Henceforth, all vehicle indices should be evaluated modulo n.

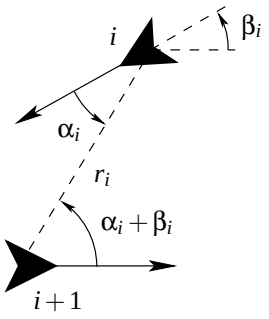

Fig. 1. New coordinates, with vehicle i in pursuit of $i+1$.

A. Transformation to Relative Coordinates

Before beginning our analysis, it is useful to consider a transformation of coordinates into ones that involve the variables r_i and α_i. We define the variables r_i, α_i, and β_i according to Fig. 1. After some (rather lengthy) algebraic manipulation, the kinematic equations (1) become

$$\begin{aligned} \dot{r}_i &= -v_i \cos\alpha_i - v_{i+1}\cos(\alpha_i+\beta_i) \\ \dot{\alpha}_i &= \frac{1}{r_i}\left[v_i \sin\alpha_i + v_{i+1}\sin(\alpha_i+\beta_i)\right] - \omega_i \\ \dot{\beta}_i &= \omega_i - \omega_{i+1}\,. \end{aligned} \tag{2}$$

This system describes the relationship between vehicle i and the one that it is pursuing, $i+1$, where r_i and α_i are as previously described. Note that, in these coordinates, it is assumed that $r_i > 0$.

B. Formation Control and Pursuit Graph

As previously suggested, we investigate the case when

$$v_i = s \quad \text{and} \quad \omega_i = k\alpha_i, \tag{3}$$

where $k, s > 0$ are constant. Substituting these controls into (2) gives a system of n cyclically interconnected and identical nonlinear subsystems of the form

$$\begin{aligned} \dot{r}_i &= -s\left[\cos\alpha_i + \cos(\alpha_i+\beta_i)\right] \\ \dot{\alpha}_i &= \frac{s}{r_i}\left[\sin\alpha_i + \sin(\alpha_i+\beta_i)\right] - k\alpha_i \\ \dot{\beta}_i &= k(\alpha_i - \alpha_{i+1})\,. \end{aligned} \tag{4}$$

At each instant in time, regardless of the control law, the multi-vehicle system's geometric configuration in the plane can be described by a *pursuit graph* as follows.

Definition 1 (Pursuit Graph): A *pursuit graph* G consists of a pair (V,E) such that

(i) V is a finite set of vertices, $|V| = n$, where each vertex $z_i = (x_i, y_i) \in \mathbb{R}^2$, $i \in \{1,\ldots,n\}$, represents the position of vehicle i in the plane; and

(ii) E is a finite set of directed edges, $|E| = n$, where each edge $e_i : V \times V \to \mathbb{R}^2$, $i \in \{1,\ldots,n\}$, is the vector from z_i to its prey, z_{i+1}.

In other words, $e_i = z_{i+1} - z_i$ and consequently $\sum_i^n e_i = 0$ for vehicles in cyclic pursuit. Also, note that our coordinate $r_i \equiv \|e_i\|_2$. We employ this definition in characterizing the equilibrium formations of our multi-vehicle system.

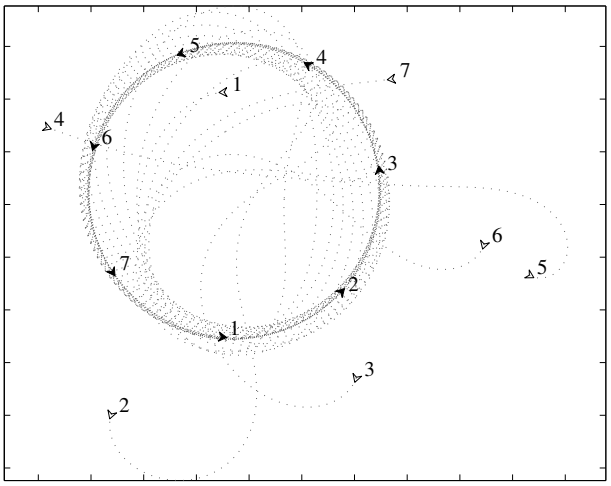

Fig. 2. Seven vehicles subject to control law (3), with $k = 4$.

C. Sample Simulation

Preliminary computer simulations suggest the possibility of achieving circular pursuit trajectories in the plane. Fig. 2 shows simulation results for a system of $n = 7$ vehicles, initially positioned at random, under the control law (3) with $k = 4$. Note that the vehicles converge to equally spaced motion around a circle of fixed radius with a pursuit graph that is similar to a regular pentagon.

III. Equilibrium Polygons

In order to characterize the possible equilibrium formations for the system (4), we need to adequately describe the state of our system's pursuit graph at equilibrium. The following definition for a regular polygon with coplanar vertices has been adapted from [11], and was introduced in [10], to allow for vertices that are not necessarily distinct and for the directed edges of our pursuit graph.

Definition 2 (after [11], p. 93): Let n and $d < n$ be positive integers so that $p := n/d > 1$ is rational. Let R be a positive rotation in the plane, about the origin, through angle $2\pi/p$ and $z_1 \neq 0$ be a point in the plane. The points $z_{i+1} = Rz_i$, $i = 1,\ldots,n-1$ and edges $e_i = z_{i+1} - z_i$, $i = 1,\ldots,n$, define a *generalized regular polygon*, denoted $\{p\}$.

By this definition, $\{p\}$ can be interpreted as a directed graph with vertices z_i (not necessarily distinct) connected by edges e_i as determined by the ordering of points.

Since p is rational, the period of R is finite and, when n and d are coprime, this definition is equivalent to the well-known definition of a regular polygon as a polygon that is both *equilateral* and *equiangular*. Moreover, when $d = 1$, $\{p = n\}$ is an *ordinary* regular polygon (i.e., its edges do not cross one another). However, when $d > 1$ is coprime to n, $\{p\}$ is a *star* polygon since its sides intersect at certain extraneous points, which are not included among the vertices [11, pp. 93–94]. If n and d have a common factor $m > 1$, then $\{p\}$ has $\tilde{n} = n/m$ distinct vertices and $\tilde{n}$ edges traversed m times. Fig. 3 illustrates some example

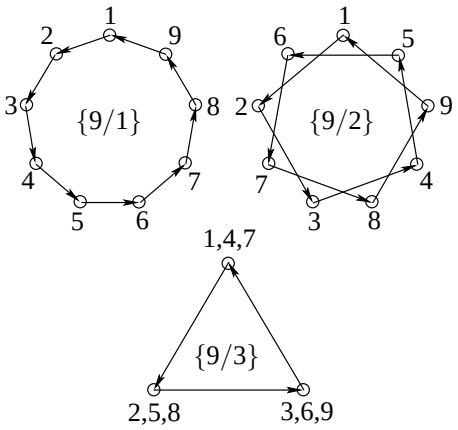

Fig. 3. Example generalized regular polygons $\{9/d\}$, $d \in \{1,2,3\}$.

possibilities for $\{p\}$ when $n = 9$. In the first instance, $\{9/1\}$ is an ordinary polygon. In the second instance, $\{9/2\}$ is a star polygon since 9 and 2 are coprime. In the third instance, the edges of $\{9/3\}$ traverse a $\{3/1\}$ polygon 3 times, because $m = 3$ is a common factor of both 9 and 3.

Theorem 1: At equilibrium, the n-vehicle pursuit graph corresponding to (4) is a generalized regular polygon $\{p\}$, where $p = n/d$ and $d \in \{1,\ldots,n-1\}$. Moreover,

$$r_i = \frac{2sn}{k\pi d}\sin\left(\frac{\pi d}{n}\right)$$

and the equilibrium angles in the range $(-\pi,\pi]$ are $\alpha_i = \pm\pi d/n$ and $\beta_i = \pm\pi(1-2d/n)$ for all $i \in \{1,\ldots,n\}$.

The proof of Theorem 1 is very similar to that of Theorem 1 in [10]. Equilibria with $\alpha_i = 0$ are not feasible for vehicles in cyclic pursuit. The case when n and d of Theorem 1 are not coprime is physically undesirable (e.g., as in the polygon $\{9/3\}$ of Fig. 3) since it requires that multiple vehicles occupy the same point in space. From geometry, it is clear that, for each possible $\{n/d\}$ formation, the equilibrium angle $\bar{\alpha} = \pm\pi d/n$ corresponds exactly to a relative heading angle for each vehicle that points it in a direction that is *tangent* to the circle circumscribed by the vertices of the corresponding equilibrium polygon.

Corollary 1: At equilibrium, the vehicles traverse a circle of radius $\rho = sn/k\pi d$.

Observe that the possible equilibrium formations depend only on our choice of gain k and forward speed s; in fact, only on the ratio $s:k$. Therefore, in what follows we assume $s = 1$ without loss of generality. Following Corollary 1, the radius about which the vehicles travel is determined by the designable parameter $k > 0$.

IV. Local Stability Analysis

In general, for $n \geq 2$, which $\{n/d\}$ equilibrium polygons are asymptotically stable, and for what values of k? In this section, we tackle the *local* stability question by linearizing about a general $\{n/d\}$ formation.

To facilitate notation, define $\tilde{\xi}_i := \xi_i - [\bar{r},\bar{\alpha},\bar{\beta}]^\top$ and let $q := p^{-1} = d/n$ so that $0 < q < 1$ and is rational. We write the kinematics of each vehicle subsystem (4) more compactly as $\dot{\xi}_i = f(\xi_i,\xi_{i+1})$. Linearizing each ξ_i model about an equilibrium point $[\bar{r},\bar{\alpha},\bar{\beta}]^\top$ gives n identical subsystems of the form $\dot{\tilde{\xi}}_i = A\tilde{\xi}_i + B\tilde{\xi}_{i+1}$ where

$$A = \begin{bmatrix} 0 & 2\sin(q\pi) & \sin(q\pi) \\ -\frac{1}{2}(kq\pi)^2\csc(q\pi) & -k & -\frac{1}{2}kq\pi\cot(q\pi) \\ 0 & k & 0 \end{bmatrix}$$

$$B = \begin{bmatrix} 0 & 0 & 0 \\ 0 & 0 & 0 \\ 0 & -k & 0 \end{bmatrix}.$$

If we view the *complete* multi-vehicle system as $\dot{\xi} = \hat{f}(\xi)$ then its linearization about $\bar{\xi} \in \mathbb{R}^{3n}$ has the form $\dot{\tilde{\xi}} = \hat{A}\tilde{\xi}$ where $\hat{A} = \mathrm{circ}[A,B,0,\ldots,0]$, defined by

$$\mathrm{circ}[A,B,0,\ldots,0] := \begin{bmatrix} A & B & 0 & 0 & \cdots & 0 \\ 0 & A & B & 0 & \cdots & 0 \\ \vdots & & & & & \\ 0 & 0 & \cdots & 0 & A & B \\ B & 0 & \cdots & 0 & 0 & A \end{bmatrix},$$

which is a matrix of *block circulant* form (cf. [12]). In the sections that follow, we study the spectrum of $\hat{A}$.

A. Coordinate Constraints

For every initial condition, the system $\dot{\xi} = \hat{f}(\xi)$ is constrained to evolve on an invariant submanifold $\mathcal{M}$ of $\mathbb{R}^{3n}$. To see why this is the case, recall that under cyclic pursuit the system's pursuit graph at each instant satisfies $\sum_{i=1}^n e_i(t) = 0$. By choosing a coordinate frame attached to (say) vehicle 1 and oriented with this vehicle's heading, this condition corresponds to the constraint equations

$$\begin{aligned} g_1(\xi) &= r_1\sin\alpha_1 + r_2\sin(\alpha_2+\pi-\beta_1) + \cdots \\ &\quad \cdots + r_n\sin(\alpha_n + (n-1)\pi - \beta_1 - \beta_2 - \cdots - \beta_{n-1}) = 0 \\ g_2(\xi) &= r_1\cos\alpha_1 + r_2\cos(\alpha_2+\pi-\beta_1) + \cdots \\ &\quad \cdots + r_n\cos(\alpha_n + (n-1)\pi - \beta_1 - \beta_2 - \cdots - \beta_{n-1}) = 0. \end{aligned}$$

For vehicles 1 and 2, Fig. 4 helps to illustrate how these constraint equations arise.

Also due to cyclic pursuit $\sum_{i=1}^n \dot{\beta}_i(t) = 0 \Longrightarrow \sum_{i=1}^n \beta_i(t) \equiv c$ for all $t \geq 0$, where the constant $c = -n\pi$ by our definition for β_i, which provides the final constraint $g_3(\xi) = \sum_{i=1}^n \beta_i + n\pi = 0$. Thus, let $g(\xi) = [g_1(\xi), g_2(\xi), g_3(\xi)]^\top$. Then it can be checked that $\mathcal{M} = \{\xi \in \mathbb{R}^{3n} : g(\xi) = 0\} \subset \mathbb{R}^{3n}$ defines a submanifold of $\mathbb{R}^{3n}$. For brevity's sake, the following are given without proof.

Lemma 1: The submanifold $\mathcal{M}$ is invariant under $\hat{f}$.

Corollary 2: Since $\mathcal{M}$ is invariant under $\hat{f}$, the tangent space $T_{\bar{\xi}}\mathcal{M}$ at any given equilibrium point $\bar{\xi} \in \mathcal{M}$ is invariant under $\hat{A}$.

Therefore, by Corollary 2 and standard results from linear algebra, there exists a change of basis for $\mathbb{R}^{3n}$ that transforms $\hat{A}$ into upper-triangular form

$$\begin{bmatrix} \hat{A}_{T_{\bar{\xi}}\mathcal{M}} & * \\ 0_{3\times(3n-3)} & \hat{A}^\star_{T_{\bar{\xi}}\mathcal{M}} \end{bmatrix}.$$

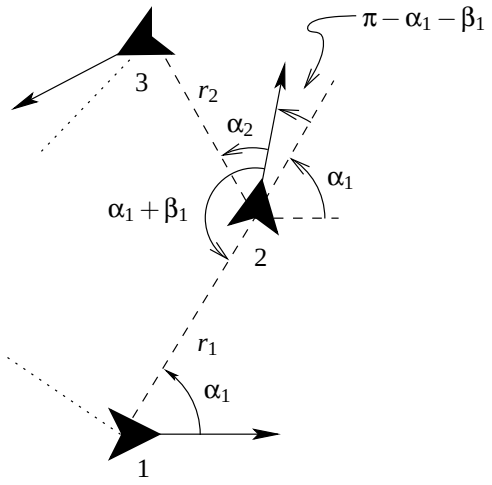

Fig. 4. Depiction of coordinates for vehicles 1 and 2.

Lemma 2: In the quotient space $\mathbb{R}^{3n}/T_{\bar{\xi}}\mathcal{M}$, the induced linear transformation $\hat{A}^{\star}_{T_{\bar{\xi}}\mathcal{M}} : \mathbb{R}^{3n}/T_{\bar{\xi}}\mathcal{M} \to \mathbb{R}^{3n}/T_{\bar{\xi}}\mathcal{M}$ has (imaginary axis) eigenvalues $\lambda_1 = 0$ and $\lambda_{2,3} = \pm jk\pi d/n$.

Proof (sketch): Let $\varphi = \Phi(\xi)$ be the coordinates change

$$\varphi_1 = r_1, \varphi_2 = \alpha_1, \ldots, \varphi_{3n-3} = \beta_{n-1}, \varphi_{3n-2} = g_1(\xi),$$
$$\varphi_{3n-1} = g_2(\xi), \varphi_{3n} = g_3(\xi)\,.$$

Partition these new coordinates into $\varphi = [\varphi_{\mathrm{I}}^{\top}, \varphi_{\mathrm{II}}^{\top}]^{\top}$ where $\varphi_{\mathrm{I}} = [\varphi_1, \varphi_2, \ldots, \varphi_{3n-3}]^{\top}$ and $\varphi_{\mathrm{II}} = [\varphi_{3n-2}, \varphi_{3n-1}, \varphi_{3n}]^{\top}$. Thus, by computing the linearization about the equilibrium $\bar{\varphi} = \Phi(\bar{\xi})$, in the new coordinates we get (details not shown)

$$\dot{\varphi}_{\mathrm{I}} = \left[\begin{array}{ccc} I_{3n-3} & 0_{(3n-3)\times 3} \end{array}\right] \hat{A}\varphi$$
$$\dot{\varphi}_{\mathrm{II}} = \left[\begin{array}{ccc|ccc} 0 & \cdots & 0 & 0 & -k\bar{\alpha} & -1 \\ 0 & \cdots & 0 & k\bar{\alpha} & 0 & 0 \\ 0 & \cdots & 0 & 0 & 0 & 0 \end{array}\right] \varphi$$
$$= \left[\begin{array}{cc} 0_{3\times(3n-3)} & \hat{A}^{\star}_{T_{\bar{\xi}}\mathcal{M}} \end{array}\right] \varphi\,.$$

The block $\hat{A}^{\star}_{T_{\bar{\xi}}\mathcal{M}}$ has eigenvalues $\lambda_{1,2,3} = 0, \pm jk\bar{\alpha}$, with $\bar{\alpha} = \pm\pi d/n$ from Theorem 1. □

Therefore, when determining the stability of a given $\{n/d\}$ polygon formation we can disregard these three imaginary axis eigenvalues of $\hat{A}$, and determine stability based on its remaining $3n-3$ eigenvalues.

B. Spectral Analysis of $\hat{A}$

In this section, we exploit the block circulant structure of $\hat{A}$ to isolate its eigenvalues. Let $\omega^{i-1} := e^{2(i-1)\pi j/n} \in \mathbb{C}$ denote the i-th of n roots of unity, where $j = \sqrt{-1}$.

Lemma 3: The matrix $\hat{A}$ can be block diagonalized into $\mathrm{diag}(D_1, D_2, \ldots, D_n)$, where $D_i = A + \omega^{i-1}B$, $i = 1, 2, \ldots, n$.

The proof of Lemma 3 follows from Theorem 5.6.4 of [12]. Therefore, each diagonal block has the same form, where $D_i = A + \omega^{i-1}B$ is given by

$$D_i = \left[\begin{array}{ccc} 0 & 2\sin(q\pi) & \sin(q\pi) \\ \frac{-1}{2}(kq\pi)^2\csc(q\pi) & -k & \frac{-1}{2}kq\pi\cot(q\pi) \\ 0 & k(1-\omega^{i-1}) & 0 \end{array}\right].$$

From Lemma 3, we observe two facts. The first is that the eigenvalues of $D_1 = A + B$ are among the eigenvalues of $\hat{A}$ for every n. The characteristic polynomial of D_1 is $p_{D_1}(\lambda) = \lambda\left(\lambda^2 + k\lambda + (kq\pi)^2\right)$. As predicted by Lemma 2, we have discovered one zero eigenvalue, while the remaining eigenvalues have $\mathrm{Re}(\lambda_{2,3}) < 0$ for every $0 < q < 1$ and $k > 0$. The second fact is that, when the number of vehicles n is even, the eigenvalues of the matrix $D_{i^*} = A - B$, with $i^* := \frac{n}{2} + 1$, are among the eigenvalues of $\hat{A}$. The characteristic polynomial of D_{i^*} is $p_{D_{i^*}}(\lambda) = \lambda^3 + k\lambda^2 + k^2\left[(q\pi)^2 + q\pi\cot(q\pi)\right]\lambda + k^3(q\pi)^2$, for which we may use the Routh-Hurwitz criterion to determine that, for stability, we would need $\cot(q\pi) > 0$, or equivalently $0 < q < \frac{1}{2}$. Moreover, in the special case when $q = \frac{1}{2}$ the characteristic polynomial factors as

$$p_{D_{i^*}}(\lambda) = \left(\lambda + j\frac{k\pi}{2}\right)\left(\lambda - j\frac{k\pi}{2}\right)(\lambda + k), \qquad (5)$$

which yields one stable and two imaginary axis eigenvalues.

Lemma 4: The stability of $\hat{A}$ is independent of $k > 0$.

Proof: Suppose we have block diagonalized $\hat{A}$ into n diagonal blocks $D_i = A + \omega^{i-1}B$ according to Lemma 3. The claim of Lemma 4 is then obvious when each block D_i is factored as $D_i = kT\tilde{D}_iT^{-1}$, where $T = \mathrm{diag}[\frac{1}{k}\sin(q\pi), 1, 1]$ (recall $0 < q < 1$) and

$$\tilde{D}_i = \left[\begin{array}{ccc} 0 & 2 & 1 \\ -\frac{1}{2}(q\pi)^2 & -1 & -\frac{1}{2}q\pi\cot(q\pi) \\ 0 & 1-\omega^{i-1} & 0 \end{array}\right]$$

so that $\sigma(D_i) = k\sigma(\tilde{D}_i)$, where $\sigma(\cdot)$ denotes the spectrum of a matrix. Since $k > 0$, the stability of the matrix $\tilde{D}_i$ implies the stability of D_i. □

Thus, whether a specific $\{n/d\}$ polygon is stable or not is independent of $k > 0$, and we can proceed by studying the blocks $\tilde{D}_i$. In other words, for a given n, only the density d influences the spectrum of $\hat{A}$.

C. Stable Equilibrium Polygons

Unfortunately, the blocks $\tilde{D}_i$ are, in general, *complex* matrices. To be explicit about this fact, we can write the n roots of unity $\omega^{i-1} = w_i + jz_i \in \mathbb{C}$, where $w_i = \cos(2\pi\frac{i-1}{n})$ and $z_i = \sin\left(2\pi\frac{i-1}{n}\right)$. In this general case, the characteristic polynomial of $\tilde{D}_i$ is $p_{\tilde{D}_i}(\lambda) = \lambda^3 + \lambda^2 + (a_2 + jb_2)\lambda + (a_3 + jb_3)$ with coefficients $a_2 = (q\pi)^2 + \frac{1}{2}q\pi(1-w_i)\cot(q\pi)$, $b_2 = -\frac{1}{2}q\pi z_i\cot(q\pi)$, $a_3 = \frac{1}{2}(1-w_i)(q\pi)^2$, and $b_3 = -\frac{1}{2}z_i(q\pi)^2$.

Theorem 2 (after Theorem 3.16 of [13, p. 180]): Consider a complex polynomial $p(\lambda) = \lambda^3 + c_1\lambda^2 + c_2\lambda + c_3$, where $c_1, c_2, c_3 \in \mathbb{C}$. Define the hermitian matrix

$$H = \left[\begin{array}{ccc} c_1 + \bar{c}_1 & c_2 - \bar{c}_2 & c_3 + \bar{c}_3 \\ -c_2 + \bar{c}_2 & \bar{c}_2 + c_2 - \bar{c}_3 - c_3 & c_3 - \bar{c}_3 \\ c_3 + \bar{c}_3 & -c_3 + \bar{c}_3 & c_2\bar{c}_3 + \bar{c}_2c_3 \end{array}\right].$$

The polynomial $p(\lambda)$ is asymptotically stable if and only if H is positive definite.

Here, $\bar{c}$ denotes the complex conjugate of c. A hermitian matrix H is positive definite if and only if its leading principal minors, denoted h_1, h_2, and h_3, are positive.

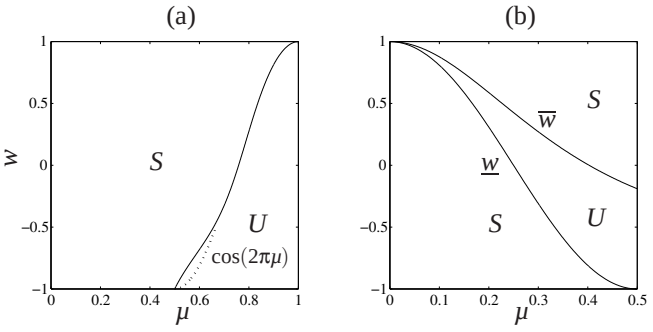

Fig. 5. Parameter w as a function of μ for the leading principal minors (a) h_2, and (b) h_3 of H. In (a), U denotes the closed set of points where $h_2 \le 0$; in (b), U denotes the closed set of points where $h_3 \le 0$.

Suppose we apply Theorem 2 to the characteristic polynomial of $\tilde{D}_i$. Computing the leading principal minors of the corresponding H gives $h_1 = 2$, $h_2 = 4(a_2 - a_3 - b_2^2)$, and $h_3 = 8(a_2^2 a_3 + a_2 b_2 b_3 - 2a_2 a_3^2 - 3a_3 b_2 b_3 - b_3^2 - a_3 b_2^2 a_2 - b_2^3 b_3 + a_3^3)$. Clearly $h_1 > 0$. Stability of a given $\tilde{D}_i$ matrix is therefore dependent on the signs of h_2 and h_3. For stability, substituting the coefficients above and using $z_i^2 = 1 - w_i^2$, we would need that

$$h_2(q, w_i) = 2(1+w_i)q\pi + 2(1-w_i)\cot(q\pi) - (1-w_i^2)q\pi\cot^2(q\pi) > 0 \tag{6}$$

for the second leading principal minor, and

$$h_3(q, w_i) = (1 + w_i - w_i^2 - w_i^3)[(q\pi)^2 + q\pi\cot(q\pi)] - (1 - w_i - w_i^2 + w_i^3)[(q\pi)^2\cot^2(q\pi) + q\pi\cot^3(q\pi)] + 2(1 - 2w_i + w_i^2)\cot^2(q\pi) - 2(1 - w_i^2) > 0$$

for the third leading principal minor. The decision to write h_2 and h_3 as functions of the real component w_i rather than the imaginary component z_i was arbitrary. In what follows, we will use these functions h_2 and h_3 to determine which $\{n/d\}$ equilibrium polygons are stable, and which are not.

For a given number of vehicles n, define the set of w_i by $\mathcal{W}_n = \{w_i = \mathrm{Re}(\omega^{i-1}) : i = 1, 2, \ldots, n\}$.

Lemma 5: Every $\{n/d\}$ equilibrium polygon with $\frac{n}{2} < d < n$ is unstable.

Proof: When n is even, we have already seen that the eigenvalues of $A - B$ (a *real* matrix) are among the eigenvalues of $\hat{A}$ (i.e., if $i^* := \frac{n}{2} + 1$, $w_{i^*} = -1$ is always a root of unity) and we have previously concluded that $D_{i^*} = A - B$ is unstable when $\frac{1}{2} < \frac{d}{n} < 1$, or equivalently $\frac{n}{2} < d < n$. When n is odd, look at h_2 and consider the set of points that are *not* stable $\mathcal{H}_2 = \{(\mu, w) : h_2(\mu, w) \le 0, \mu \in (0,1), w \in (-1,1)\}$, which is illustrated by region U of Fig. 5a. Note that we are taking μ and w on a continuum, whereas the arguments of h_2 in (6), q and $w_i \in \mathcal{W}_n$, take on rational and discrete values, respectively. Let $\mathrm{int}\mathcal{H}_2$ denote the interior of $\mathcal{H}_2$. It is a fact that the pair $(\mu, \cos(2\pi\mu)) \in \mathrm{int}\mathcal{H}_2$ for every $\mu \in (\frac{1}{2}, \frac{2}{3}]$, as illustrated by the dotted line in Fig. 5a. This fact, which is most easily checked numerically, will be useful in what follows. Let $d^* := \frac{n+1}{2}$, the smallest integer satisfying the condition $\frac{n}{2} < d < n$ of the lemma. Let $i^* := d^* + 1$, which gives $w_{i^*} = \mathrm{Re}(\omega^{d^*}) = \cos(2\pi\frac{d^*}{n}) \in \mathcal{W}_n$. Note that $\frac{1}{2} < \frac{d^*}{n} \le \frac{2}{3}$ for every $n \ge 3$, which (by the previously stated fact) implies that for every $n \ge 3$ there exists a $w_{i^*} \in \mathcal{W}_n$ such that $(\frac{d^*}{n}, w_{i^*}) \in \mathrm{int}\mathcal{H}_2$, i.e., every $\{n/d^*\}$ polygon is unstable. It is left to show that the remaining densities $d^* < d < n$ satisfying the condition $\frac{n}{2} < d < n$ of the lemma are also unstable. Since $\frac{d^*}{n} < \frac{d}{n} < 1$, the point $(\frac{d}{n}, w_{i^*}) \in \mathrm{int}\mathcal{H}_2$ also lives in the region U. This is because it lies directly to the right of the unstable point $(\frac{d^*}{n}, w_{i^*}) \in \mathrm{int}\mathcal{H}_2$ in Fig. 5a, which concludes the proof. □

Before stating our main result, consider the set of points that are *not* stable $\mathcal{H}_3 = \{(\mu, w) : h_3(\mu, w) \le 0, \mu \in (0, \frac{1}{2}], w \in (-1, 1)\}$, which is illustrated by the region U of Fig. 5b. Define the following functions

$$\overline{w}(\mu) := \frac{2\tan(\mu\pi)}{\mu\pi[1 + \mu\pi\tan(\mu\pi)]} - 1$$
$$\underline{w}(\mu) := \cos(2\pi\mu),$$

which describe the upper and lower boundaries of the region U in Fig. 5b. These functions were obtained by solving the equation $h_3(\mu, w) = 0$ on the relevant domain $\mu = (0, \frac{1}{2}]$ and $w \in (-1, 1)$ and numerically checking that the region U indeed corresponds to the set $\mathcal{H}_3$. As a result, the definition given above for $\mathcal{H}_3$ is equivalent to $\mathcal{H}_3 = \{(\mu, w) : \mu \in (0, \frac{1}{2}], w \in [\underline{w}(\mu), \overline{w}(\mu)]\}$.

Theorem 3 (Main Stability Result): An $\{n/d\}$ equilibrium polygon is locally asymptotically stable if and only if $0 < d \le \frac{n}{2}$ and $\underline{w}(\frac{d-1}{n}) > \overline{w}(\frac{d}{n})$.

Proof: According to the proof of Lemma 5, $h_2 < 0$ for every $\{n/d\}$ polygon with $\frac{n}{2} < d < n$. Thus, a necessary condition for stability is that $0 < d \le \frac{n}{2}$.

Notice that $h_2 > 0$ for every $0 < d < \frac{n}{2}$ (see Fig. 5a). Let's proceed by assuming that this condition holds for the given $\{n/d\}$ polygon. We will consider the special case when $d = \frac{n}{2}$ separately. Observe that every matrix D_i has a complex conjugate matrix D_{n-i+2}, hence the spectra of D_i and its conjugate are also complex conjugates. Define $i^* := d + 1$ so that $w_{i^*} = \cos(2\pi\frac{d}{n}) \equiv \underline{w}(\frac{d}{n})$. Thus, the point $(\frac{d}{n}, w_{i^*})$ lies exactly on the lower boundary of $\mathcal{H}_3$ in Fig. 5b. Together, the matrix D_{i^*} and its conjugate D_{n-i^*+2} have two imaginary axis eigenvalues (one each) of the form $\lambda = \pm jk\pi\frac{d}{n}$, while the remaining eigenvalues have $\mathrm{Re}(\lambda) \ne 0$. These facts were verified with the assistance of computer algebra software. The eigenvalues with $\mathrm{Re}(\lambda) \ne 0$ cannot be unstable, otherwise the point $(\frac{d}{n}, w_{i^*})$ would not lie on the boundary of $\mathcal{H}_3$. According to Lemma 2, we can disregard the two imaginary axis eigenvalues, and also the zero eigenvalue of D_1, since they have no connection to the stability of the given $\{n/d\}$ polygon. Since the point $(\frac{d}{n}, w_{i^*})$ lies on the lower boundary of $\mathcal{H}_3$, all points $(\frac{d}{n}, w_i)$, $w_i \in \mathcal{W}_n$ with $w_i < w_{i^*}$ lie outside the unstable set $\mathcal{H}_3$. Thus, we turn our attention to the points $(\frac{d}{n}, w_i)$, $w_i \in \mathcal{W}_n$ with $w_i > w_{i^*}$. Define the index $i' := i^* - 1 = d$, corresponding to $w_{i'} \in \mathcal{W}_n$, $w_{i'} > w_{i^*}$ that is *closest* to w_{i^*}. This new value is given by $w_{i'} = \cos(2\pi\frac{d-1}{n}) \equiv \underline{w}(\frac{d-1}{n})$. If $w_{i'} > \overline{w}(\frac{d}{n})$, then

TABLE I

EQUILIBRIUM POLYGONS WITH STABLE POLYGONS SHADED.

$d=1$	2	3	4	5	6
$\{2/1\}$	$\{3/2\}$	$\{4/3\}$	$\{5/4\}$	$\{6/5\}$	$\{7/6\}$
$\{3/1\}$	$\{4/2\}$	$\{5/3\}$	$\{6/4\}$	$\{7/5\}$	$\{8/6\}$
$\vdots$	$\vdots$	$\vdots$	$\vdots$	$\vdots$	$\vdots$
$\{7/1\}$	$\{8/2\}$	$\{9/3\}$	$\{10/4\}$	$\{11/5\}$	$\{12/6\}$
$\{8/1\}$	$\{9/2\}$	$\{10/3\}$	$\{11/4\}$	$\{12/5\}$	$\{13/6\}$
$\vdots$	$\vdots$	$\vdots$	$\vdots$	$\vdots$	$\vdots$
$\{17/1\}$	$\{18/2\}$	$\{19/3\}$	$\{20/4\}$	$\{21/5\}$	$\{22/6\}$
$\{18/1\}$	$\{19/2\}$	$\{20/3\}$	$\{21/4\}$	$\{22/5\}$	$\{23/6\}$
$\vdots$	$\vdots$	$\vdots$	$\vdots$	$\vdots$	$\vdots$
$\{49/1\}$	$\{50/2\}$	$\{51/3\}$	$\{52/4\}$	$\{53/5\}$	$\{54/6\}$
$\{50/1\}$	$\{51/2\}$	$\{52/3\}$	$\{53/4\}$	$\{54/5\}$	$\{55/6\}$
$\vdots$	$\vdots$	$\vdots$	$\vdots$	$\vdots$	$\vdots$

the point $(\frac{d}{n}, w_i) \notin \mathcal{H}_3$ for all $w_i \in \mathcal{W}_n$, $w_i > w_{i^*}$. Therefore, by Theorem 2, stability is equivalent to $\underline{w}(\frac{d-1}{n}) > \overline{w}(\frac{d}{n})$.

Now, in the special case when $d = \frac{n}{2}$, the matrix D_{i^*} is *real* and has eigenvalues according to the roots of (5), as shown on page 4. Therefore, one is stable and the remaining two imaginary axis eigenvalues should be ignored according to Lemma 2. The rest follows as for $0 < d < \frac{n}{2}$. □

The following of corollary (given without proof) employs this main result to explicitly disclose which $\{n/d\}$ equilibrium polygons are stable and which are not.

Corollary 3: Following Theorem 3: (i) every $\{n/1\}$ polygon is locally asymptotically stable; (ii) every $\{n/2\}$ polygon with $n \geq 4$ is locally asymptotically stable; (iii) every $\{n/d\}$ polygon with $d \geq 6$ is unstable; (iv) for a $\{n/d\}$ polygon with $d \in \{3,4,5\}$, let $\bar{\mu}$ be the unique solution to $\underline{w}\left(\mu - \frac{\mu}{d}\right) = \overline{w}(\mu)$; then $\{n/d\}$ is locally asymptotically stable if and only if $d < \bar{\mu} n$.

Thus, we find that polygon $\{10/3\}$ is stable, while $\{9/3\}$ is not. Similarly, $\{21/4\}$ is stable, while $\{20/4\}$ is not, and finally $\{54/5\}$ is stable, while $\{53/5\}$ is not. Table I lists all possible equilibrium polygons with $1 \leq d \leq 6$ and gives their local stability.

D. Sample Simulations

Fig. 2 and Fig. 6 show computer simulation results for $n = 7$ vehicles, where in each case the forward speed $s = 1$ and gain $k = 4$. However, due to differing initial conditions, the vehicles of Fig. 2 form a $\{7/1\}$ polygon at equilibrium, whereas the vehicles of Fig. 6 converge to a $\{7/2\}$ equilibrium formation.

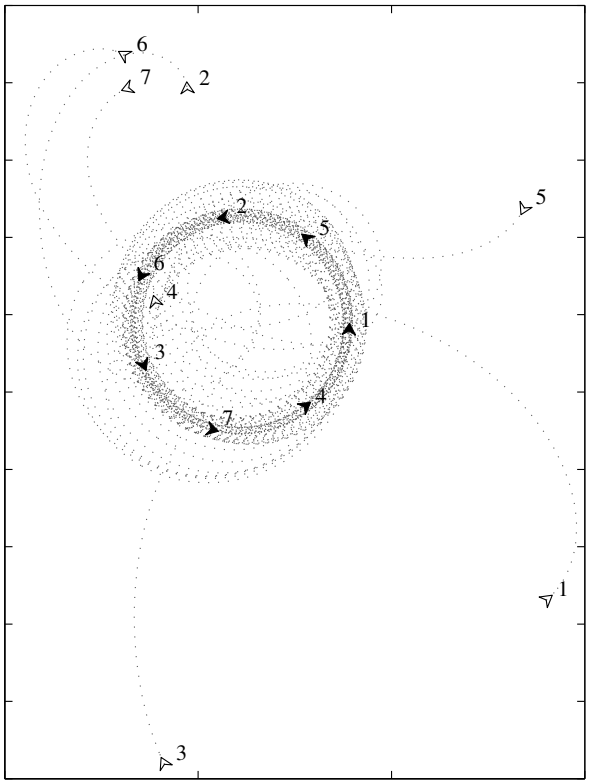

Fig. 6. Unicycles in cyclic pursuit generating a $\{7/2\}$ formation.

REFERENCES

[1] E. W. Justh and P. S. Krishnaprasad, "Steering laws and continuum models for planar formations," in *Proceedings of the 42nd IEEE Conference on Decision and Control*, Maui, Hawaii, December 2003, pp. 3609–3614.

[2] A. Jadbabaie, J. Lin, and A. S. Morse, "Coordination of groups of mobile autonomous agents using nearest neighbor rules," *IEEE Transactions on Automatic Control*, pp. 988–1001, June 2003.

[3] V. Gazi and K. M. Passino, "Stability analysis of swarms," in *Proceedings of the American Control Conference*, Ancharage, Alaska, May 2002, pp. 1813–1818.

[4] R. Sepulchre, D. Paley, and N. Leonard, "Collective motion and oscillator synchronization," to appear in *Proceedings of the 2003 Block Island Workshop on Cooperative Control*, Springer-Verlag LNCIS Series, 2004.

[5] A. Bernhart, "Polygons of pursuit," *Scripta Mathematica*, vol. 24, pp. 23–50, 1959.

[6] M. S. Klamkin and D. J. Newman, "Cyclic pursuit or "The three bugs problem"," *The American Mathematical Monthly*, vol. 78, no. 6, pp. 631–639, June/July 1971.

[7] F. Behroozi and R. Gagnon, "Cylcic pursuit in a plane," *Journal of Mathematical Physics*, vol. 20, no. 11, pp. 2212–2216, 1979.

[8] T. J. Richardson, "Non-mutual captures in cyclic pursuit," *Annals of Mathematics and Artificial Intelligence*, vol. 31, pp. 127–146, 2001.

[9] A. M. Bruckstein, N. Cohen, and A. Efrat, "Ants, crickets and frogs in cyclic pursuit," Technion-Israel Institute of Technology, Haifa, Israel, Center for Intelligent Systems technical report #9105, July 1991.

[10] J. A. Marshall, M. E. Broucke, and B. A. Francis, "A pursuit strategy for wheeled-vehicle formations," in *Proceedings of the 42nd IEEE Conference on Decision and Control*, Maui, Hawaii, December 2003, pp. 2555–2560.

[11] H. S. M. Coxeter, *Regular Polytopes*. London: Methuen & Co. Ltd., 1948.

[12] P. J. Davis, *Circulant Matrices*, 2nd ed. New York: Chelsea Publishing, 1994.

[13] S. Barnett, *Polynomials and Linear Control Systems*, ser. Monographs and Textbooks in Pure and Applied Mathematics Series. New York: Marcel Dekker, Inc., 1983.